satisfies the requirement for low-voltage-operated frequency-hopping spread-spectrum (FH-SS) application [6].

ACKNOWLEDGMENT

This work was supported by Strategic Grant no. 7001422 of the City University of Hong Kong.

REFERENCES

1. V.F. Kroupa, Noise properties of PLL systems, IEEE Trans Commun COM-30 (1982).
2. A. Kajiwara, A new PLL frequency synthesizer with high switching speed, IEEE Trans Vehic Technol 41 (1992), 407–413.
3. F.M. Gardner, Charge-pump phase-lock loops, IEEE Trans Commun COM-28 (1980), 1849–1858.
4. F.M. Gardner, Phase accuracy of charge pump PLLs, IEEE Trans Commun COM-28 (1980), 2362–2363.
5. J.A. Connely and K.P. Taylor, An analysis methodology to identify dominant noise sources in D/A and A/D converter, IEEE Trans Circ Syst 38 (1991).
6. FCC Regulation, Part 15.247.

EFFECTS OF Ge CONCENTRATION, BORON CO-DOPING, AND HYDROGENATION ON FIBER BRAGG GRATING CHARACTERISTICS

M. Konstantaki,[1] G. Tamiolakis,[1] A. Argyris,[2] A. Othonos,[3] and A. Ikiades[4]

[1] Foundation for Research and Technology-Hellas (FORTH)
IESL
PO Box 1527
71110 Crete, Greece
[2] Department of Informatics
University of Athens
15784 Athens, Greece
[3] Department of Physics
University of Cyprus
PO Box 20537
Nicosia, CY-1678, Cyprus
[4] Department of Physics
University of Ioannina
PO Box 45110
Ioannina, Greece

Received 30 June 2004

ABSTRACT: *In this paper, we compare photosensitivity, refractive-index modulation depth, spectral bandwidth, and excess loss through the inscription of fiber Bragg gratings in unloaded and hydrogen-loaded fibers with low- or high-germanium concentration and boron co-doping. Gratings in hydrogenated boron co-doped fibers possess the highest reflectivity, but with wider bandwidth and strong excess loss.* © 2004 Wiley Periodicals, Inc. Microwave Opt Technol Lett 44: 148–152, 2005; Published online in Wiley InterScience (www.interscience.wiley.com). DOI 10.1002/mop.20572

Key words: *optical fiber; Bragg grating; boron co-doping; hydrogenation; optical device*

1. INTRODUCTION

Fiber Bragg gratings (FBGs) have become a significant key component in the continuously evolving fields of optical communications and optical-fiber sensing, performing a variety of essential functions. Since Hill et al. [1] reported on the convenient method of writing FBGs, based on the near-contact exposure of the fiber through a phase mask, various aspects of grating characteristics and potential applications have been investigated.

TABLE 1 Examined Fibers Listed with Their Germanium Concentration and the Code Names Used in This Paper

Code Name	Fiber Design	Ge Concentration
Ge	Low-loss germanosilica fiber	5 mol %
High Ge	High-index germanosilica fiber	20 mol %
B/Ge	Boron co-doped fiber	~20 mol %
Hydro Ge	Hydrogenated low-loss germanosilica fiber	5 mol %
Hydro High Ge	Hydrogenated high-index germanosilica fiber	20 mol %
Hydro B/Ge	Hydrogenated boron co-doped fiber	~20 mol %

Most applications require gratings of high reflectivity; thus, fiber photosensitivity is an important factor in the development of specific FBGs. For example, dense wavelength division multiplexing (DWDM) systems with 8, 16, or more channels are used to cope with increasing demand for transmission capacity. These channels can be defined by multiple, superimposed [2] FBGs that require highly photosensitive fibers for efficient inscription. Ideally, photosensitivity should be directly proportional to the reflectivity of the inscribed grating and the modulation depth should be the same or larger than the average index change for fiber exposed to maximum-contrast grating-diffraction patterns. However, the depth-to-average index change depends on the fiber type, since it is influenced by intrinsic factors such as the nonlinearities in the photosensitive response of the fiber [1].

Additionally, FBG characteristics such as bandwidth and excess loss affect its performance as a system component and must be tuned to suite each specific application. FBGs used as wavelength-selective channel dropping or inserting filters [3] must have very narrow spectral widths, whereas when used for dispersion compensation [4], broadband FBGs are required. The background loss can be detrimental, thus decreasing the reflectivity saturation value at the Bragg wavelength, increasing the out-of-band transmission loss, and broadening the reflectivity spectrum.

The photosensitivity of a variety of fibers has been investigated and compared (for a review, see [5]), including germanosilica fibers with standard or increased germanium concentration and fibers with dopands such as boron or deuterium. Usually, the photosensitivity of these special fibers is enhanced by the incorporation of extra Ge doping, which varies from 15% mol to 25% mol, depending on the manufacturer. Boron co-doping is normally used to lower the NA of the Ge-enriched fibers. Boron co-doped fiber has an excellent photosensitive response—much greater than a fiber with an equivalent germanium concentration [6]. Hydrogen loading is often used to generate or significantly enhance the photosensitivity of various types of optical fibers and high reflectivities have been reported with hydrogenated boron co-doped fibers. However, there is insufficient information on the additional characteristics of the FBG inscribed in different fiber types. Furthermore, the variability of inscription conditions and photosensitization processes makes direct comparison of the effect of hydrogenation according to fiber types obtained from different studies rather difficult.

In this paper, a direct comparison of photosensitivity, refractive-index modulation depth, bandwidth, and excess loss is presented for three different fibers. The examined fibers, described in Table 1, are a germanosilica fiber with low-Ge concentration and two similar high-Ge concentration fibers, one of which was boron

co-doped. This choice of fibers allows the investigation of the effect of the germanium concentration and boron co-doping upon the characteristics of the inscribed gratings. Samples of the three fibers were hydrogenated using identical conditions and the results offer an insight on the effect of hydrogenation upon different fiber types.

2. EXPERIMENTS

For the inscription of the FBGs, a 25-mm-long phase mask with a pitch length of 1059.7 nm was used [1]. A KrF Excimer laser was employed, emitting pulses with 20-ns duration at 248 nm. The beam profile had a rectangular shape with dimensions of 31 × 14 mm^2 and was focused to half of its original height by a cylindrical lens. The fiber was placed almost in contact with the phase mask and along the line of maximum intensity of the focused beam. The laser fluence incident on the fiber was 92 mJ/cm^2 per pulse with pulse repetition rates of 2 to 10 Hz. A rectangular aperture with controllable width was placed in front of the phase mask to control the grating length. This was deemed necessary in order to reduce the edge effects of the UV beam that may result in the inscription of an apodized FBG.

To allow on-line monitoring of the inscription process, the fluorescence of an erbium-doped fiber was used as a broadband source. The photosensitive fibers were spliced on one of the output ports of a 3-dB coupler, thus enabling the simultaneous measurement of the reflected and transmitted spectra using an optical spectral analyzer. During the inscription of the FBG, information on the evolution of the Bragg wavelength and its spectral full-width half-maximum (FWHM) was recorded from the reflected signal, while the reflectivity of the FBG was calculated through the power decrease observed in the transmission spectrum at the Bragg wavelength.

The fibers used for the UV inscription of the FBGs are listed in Table 1 along with the code names used for their description in this paper. Hydrogenation was achieved by placing samples of the fibers in a hydrogen chamber at 160-atm pressure and ambient temperature for 30 days. Bragg gratings were written immediately after removal from the chamber, before any significant out-diffusion of hydrogen could occur.

3. RESULTS AND DISCUSSION

The UV induced change in the mean refractive index of a fiber (Δn), and thus its photosensitivity, can be deduced by measuring the shift of the central Bragg wavelength during FBG inscription. Initially, the fiber is exposed to a single laser pulse and a very weak grating is inscribed with a central Bragg wavelength λ_0. Then the inscription procedure is continued and the instantaneous central Bragg wavelength λ_i is measured at constant time intervals (1 min). The refractive index change at each interval can be calculated using the Bragg condition [1]:

$$\Delta n_i = \frac{\lambda_i - \lambda_0}{2\Lambda}, \tag{1}$$

where Λ is the period of the Bragg grating. Using this method, the evolution of the refractive index change Δn was calculated for gratings inscribed in all fibers under examination, with and without hydrogenation, and the results are illustrated in Figure 1.

As can be seen from Figure 1, the photoinduced refractive index change for the low-loss germanosilica fiber (Ge) is, as expected, the lowest among the fibers examined. The high-index germanosilica (High Ge) and the boron co-doped (B/Ge) fibers exhibit similar behavior, with the boron co-doped fiber being

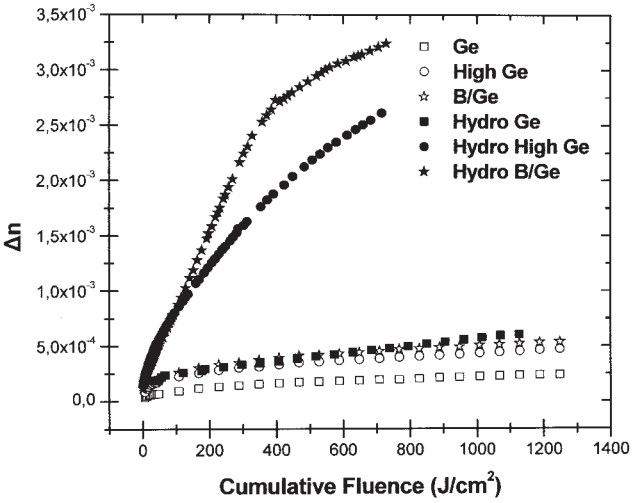

Figure 1 Evolution of photo-induced refractive-index changes for different fibers and the effect of hydrogenation (code names used are explained in Table 1)

slightly (10%) more photosensitive. Both fibers reach saturation above 200 J/cm^2, with a refractive index change of 3.8×10^{-4} for the High Ge and 4.5×10^{-4} for the B/Ge, increasing very slowly thereafter.

Hydrogenation has a minimum effect on the Ge fiber, increasing its photosensitivity only by a factor of 2.5. On the contrary, in the case of High Ge and B/Ge fibers, hydrogenation has a marked effect, thus increasing their photosensitivity significantly. Specifically, for accumulative fluences up to 150 J/cm^2, both fibers exhibit the same rapid increase in the refractive index. For longer exposure times, the refractive-index change of the hydrogenated boron co-doped fiber (Hydro B/Ge) continues to increase at the same rate, showing signs of saturation only above 400 J/cm^2, while for the hydrogenated high-index germanosilica fiber (Hydro high Ge), the increase is much slower. Particularly, for an accumulate fluence of 750 J/cm^2, the Hydro high Ge fiber exhibits an index change of 2.6×10^{-3} with the corresponding value for the Hydro B/Ge fiber being around 3.2×10^{-3}, which are almost an order of magnitude higher, as compared to the unloaded fibers. Longer irradiation of the fibers in both cases resulted in a decrease of the bandwidth and a slow erasure of the grating, thus indicating, possibly, the inscription of type IIA FBG.

During the inscription of the FBGs, the change in the refractive index also manifests as an increase in the bandwidth of the inscribed gratings. The evolution of the FWHM spectral bandwidth of the FBGs is given in Figure 2 for High Ge and B/Ge fibers. For accumulative fluence up to 1200 J/cm^2, the linewidth of FBGs inscribed in unloaded fibers does not exceed 0.30 nm. Similar behavior was observed for hydrogenated low loss germanosilica fiber (not shown in the graph) reaching only slightly higher linewidths. In contrast, for Hydro high Ge and Hydro B/Ge fibers much broader FBGs could be inscribed. Specifically, for an accumulative fluence of 750 J/cm^2, the bandwidth of the grating inscribed in the Hydro high Ge fiber is 2.4 nm. For the same conditions using Hydro B/Ge fiber, much broader FBGs are produced with FWHM equal to 4.3 nm.

From these results, we observe that, for unloaded fibers, boron co-doping increases the photosensitivity only slightly, since the refractive-index change observed in the High Ge fiber is only 1.2 times higher than that in Ge fibers. The germanium concentration of the fiber and the presence of boron dopands affects the response

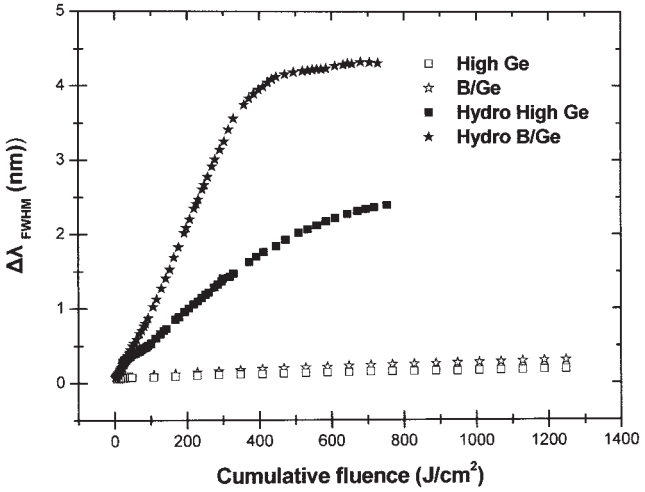

Figure 2 Evolution of FWHM bandwidth of the inscribed gratings with increasing cumulative radiation fluence

of the fiber to hydrogenation, as manifested through the characteristics of the FBGs inscribed in different hydrogenated fibers. Although hydrogen loading only doubles the photosensitivity of Ge fiber, the effect is much stronger (almost by an order of magnitude) in fibers with high germanium concentration. Hydrogenation with the presence of boron co-dopands in the fiber core significantly enhances the photo-induced increase rate of the refractive index. Additionally, the bandwidth of the inscribed gratings is almost double that of FBGs inscribed in germanosilica fibers without boron.

The refractive-index change calculated through the shift of the Bragg wavelength during inscription, using Eq. (1), is the average-refractive-index change that occurs along the length of the grating and corresponds schematically to Δn_{AV} in Figure 3. It includes the refractive-index modulation that produces the grating and a background index change encountered along the entire length of the exposed fiber. The refractive-index modulation corresponds schematically to Δn_{MOD} in Figure 3. The modulation to average refractive index ratio, $\Delta n_{MOD}/\Delta n_{AV}$, is influenced by many factors, such as less-than-perfect nulling of the zero-order beam by the phase mask, the presence of higher-order diffracted beams downstream from the mask, and the low coherence of the laser source [1]. All the above factors depend upon the experimental setup and therefore are present equally in FBGs inscribed with identical conditions, even in different fibers. The factor that is unique for each fiber is the nonlinearities in the photosensitivity

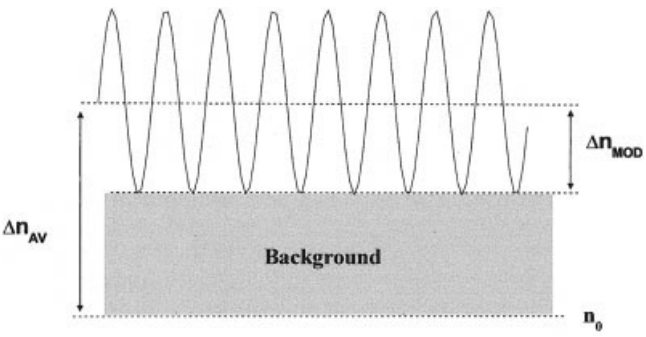

Figure 3 Graphical representation the modulation Δn_{MOD} and the average refractive-index change Δn_{AV} of a grating

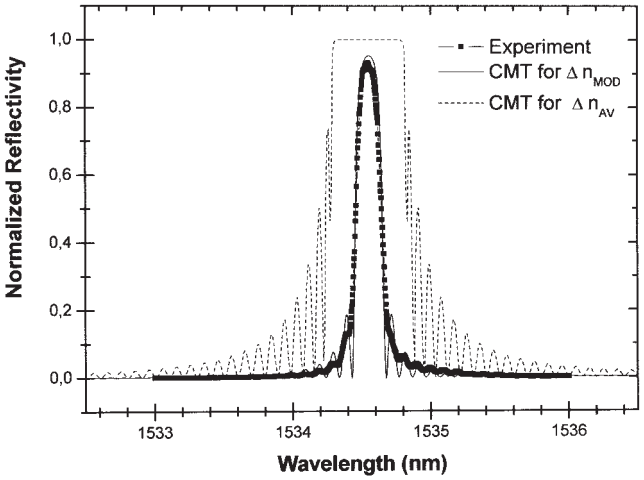

Figure 4 Comparison of experimental data with two theoretically predicted reflection spectra using the modulation Δn_{MOD} and the average Δn_{AV} refractive-index change respectively for an 8-mm-long grating in a boron co-doped fiber

response and the fiber–mask alignment. Careful experimental procedures can minimize the effect of the latter; consequently, comparison of the modulation to average refractive index ratio, $\Delta n_{MOD}/\Delta n_{AV}$, for different fibers can provide additional information on their suitability in FBG inscription.

For the determination of the refractive-index modulation, we employ the coupled-mode theory (CMT) [7]. According to theoretical analysis, the index modulation Δn_{MOD} for a grating of length L, that is uniform along its length, can be calculated from the equation for reflectivity R [7]:

$$R = \frac{\sinh^2(\sqrt{\kappa^2 - \hat{\sigma}^2}\, L)}{\cosh^2(\sqrt{\kappa^2 - \hat{\sigma}^2}\, L) - \dfrac{\hat{\sigma}^2}{\kappa^2}}, \tag{2}$$

with

$$\kappa = \frac{\pi}{\lambda}\, \upsilon \Delta n_{MOD}, \qquad \hat{\sigma} = \beta - \frac{\pi}{\Lambda} + \frac{2\pi}{\lambda}\, \Delta n_{MOD},$$

where υ is the optical-fringe visibility, assumed to be constant and close to 1 for all the inscribed gratings, β is the mode-propagation constant, and Λ is the nominal period of the FBG.

For a grating of 8-mm length, written in a B/Ge fiber with a reflectivity of 92%, the average index change Δn_{AV} measured experimentally using Eq. (1) is 4.5×10^{-4}. If one uses this value in Eq. (2) and attempts to theoretically predict the reflection spectrum of the grating, the result does not agree with the experimental data, as can be seen from Figure 4. If, however, we treat Δn_{MOD} in Eq. (2) as an unknown and attempt a fitting of the experimental reflection curve, for a value of $\Delta n_{MOD} = 1.5 \times 10^{-4}$, an almost perfect match between experiment and CMT occurs. Therefore, the modulation to average refractive index ratio, $\Delta n_{MOD}/\Delta n_{AV}$, for this grating is around 0.33.

To determine the effect of grating length and cumulative inscription fluence on the $\Delta n_{MOD}/\Delta n_{AV}$ value, we inscribed Bragg gratings of different length using a slit of controllable width positioned in front of the mask. For three different accumulate inscription fluences 464 J/cm^2, 110 J/cm^2 and 22 J/cm^2 three different average index changes Δn_{AV} are induced and the results

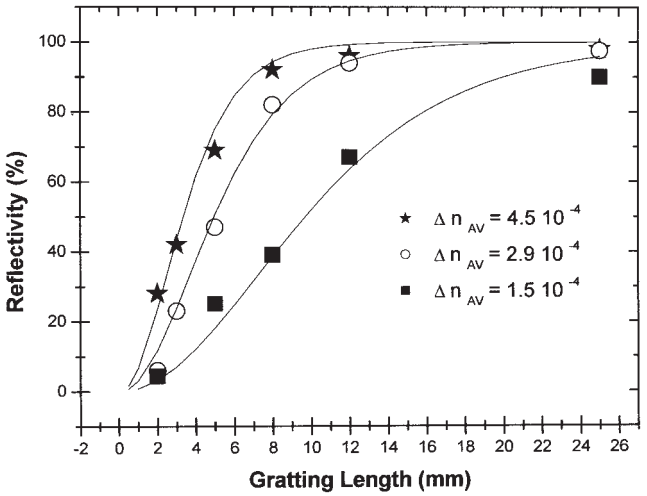

Figure 5 Grating reflectivities vs. grating length for three different accumulate inscription fluences (solid lines represent a theoretical fit)

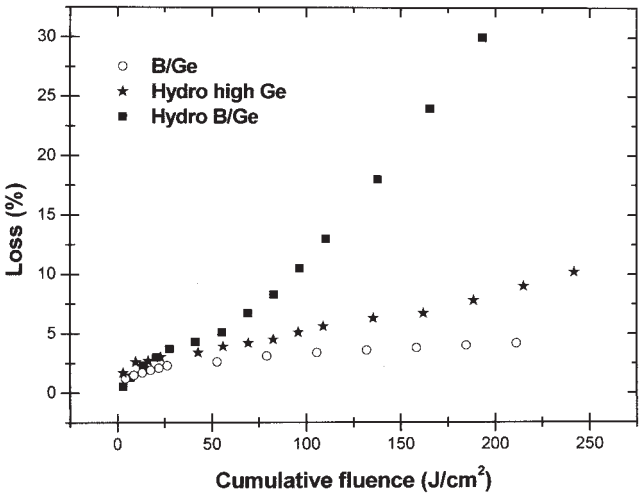

Figure 6 Excess loss of FBGs vs. cumulative fluence for three different fibers

are shown in Figure 5. The solid lines represent the theoretical fit of the following equation [7]:

$$R_{BRAGG} = \tan^2 h(\kappa L), \tag{3}$$

where R_{BRAGG} is the maximum reflectivity at the Bragg wavelength and κ is as previously defined in Eq. (2). In κ, the value of Δn_{MOD} emerges from Δn_{AV} using the 0.33 value for $\Delta n_{MOD}/\Delta n_{AV}$ in all cases. The good agreement between theoretical and experiment results suggests that for the same fiber, $\Delta n_{MOD}/\Delta n_{AV}$ is constant regardless of grating length and strength. This reinforces our initial postulation that $\Delta n_{MOD}/\Delta n_{AV}$ is affected only by the photosensitivity response of the fiber and not by the additional factors listed in the previous paragraph.

The calculations were repeated for the other fibers under examination and the results are summarized in Table 2. As can be seen, the increase in photosensitivity is accompanied by an increase in the modulation index. The highest value of $\Delta n_{MOD}/\Delta n_{AV}$, around 0.45, is obtained for the Hydro B/Ge fiber, which indicates that hydrogenation of boron co-doped fiber enhances the photo-induced modulation refractive index, thus making this type of fiber the best candidate for the inscription of high-reflectivity FBGs.

High reflectivity is a desired characteristic of FBGs, as is low background loss, which suffers during UV exposure and reduces both the grating reflectivity and the total transmission of the fiber. In this paper, the losses are calculated by comparing the transmitted signal at constant time intervals during inscription with the signal recorded for the unexposed fiber. The measurement is carried out at a wavelength higher than the Bragg wavelength (where the losses experienced are higher than at the short wavelength side [8]) and sufficiently far to exclude the effect of the side lobs.

TABLE 2 Modulation to Average Refractive Index Ratio $\Delta n_{MOD}/\Delta n_{AV}$ for Different Fibers

Fiber Design	$\Delta n_{MOD}/\Delta n_{AV}$ ($\pm$0.02)
High Ge	0.30
B/Ge	0.33
Hydro High Ge	0.37
Hydro B/Ge	0.45

Figure 6 shows the increase in the loss measured experimentally, as described above, for different fibers and for increasing accumulative inscription fluence. As can be seen losses are very low for the non-hydrogenated fibers. For the High Ge fiber (not shown in the graph) the losses were negligible while for the B/Ge fiber losses are kept below 5% up to the saturation of the photosensitivity. For the hydrogenated fibers, losses are much more significant especially in the case of Hydro B/Ge fibers. A sharp increase of loss is observed for accumulate inscription fluence above 50 J/cm^2. For an accumulate inscription fluence of 200 J/cm^2 losses approach 30%, indicating fiber damage. In the case of Hydro high Ge fibers the effect of loss is not so pronounced and for the range of accumulate fluences examined (up to 250 J/cm^2) losses reach a maximum value of 10%.

In summary, the hydrogenated boron co-doped fiber possesses the highest photosensitivity and refractive-index modulation among the fibers examined in this work, but with the inscribed FBGs exhibiting relatively wide bandwidth and high levels of excess loss. Moreover, a fiber with the same germanium concentration but without the presence of boron gave lower photo-induced refractive-index change and refractive-index modulation, but the losses measured were much lower and the FBGs spectrally narrower. Therefore, the choice of the appropriate fiber for FBG inscription depends upon the application.

Although it is beyond the scope of this work to examine the physical mechanics behind the observed photosensitivity response, we can comment that in spite of the significant advantages in the fabrication technology and the application of the FBG, the origin of photosensitivity is not well understood. Although boron co-doping used in conjunction with high-Ge concentration aims to reduce the numerical aperture of the fiber, it has a profound effect upon the photosensitivity as well as the FBG inscription dynamics. Suggestions as to the cause of the enhanced photosensitivity in boron co-doped fibers include photo-induced stress relaxation instigated by the breaking of the bonding defect responsible for the 240-nm peak [6] and increased number of Si-Ge oxygen deficiency centers prompted by the improved mixing of the glass components [9] due to the presence of boron. Additionally, a proposed model for the UV-induced reaction in GeO_2-doped glass in the presence of H_2 [10] involves H_2 molecules reacting at normal Si-O-Ge sites,

thus resulting in the formation of OH species and UV-bleachable GeO_2 deficiency centers, which are responsible for the enhanced photosensitivity. It has also been suggested [11] that hydrogenation of boron co-doped germanosilica fiber induces a permanent reduction of axial stress in the fiber's core. This stress relief is due to reactions between hydrogen molecules and drawing-induced defects (DIDs).

Based on the above reports and the results presented here, we postulate that the different photosensitivity-enhancement mechanisms observed individually due to boron co-doping and hydrogenation contribute additively to the final photosensitivity in hydrogenated boron-doped fibers. Furthermore, the contribution appears to be nonlinear. However, additional investigations on the spectroscopy of the inscription process are required in order to establish the degree of involvement of the different mechanisms.

4. CONCLUSION

We have presented a direct comparison of the characteristics such as photo-induced refractive-index change, FWHM bandwidth, refractive-index modulation, and excess loss of fiber Bragg gratings (FBGs) inscribed in three different fibers. The fibers examined are a germanosilica fiber with low-Ge concentration and two fibers with similar high-Ge concentration, one of which is boron co-doped. Additionally, samples hydrogenated using identical conditions were examined to gain an insight on the effect of hydrogenation on different fiber types. The results demonstrate that the characteristics of the FBGs depend critically on the type of fiber.

A comparison of the photo-induced refractive-index change and its evolution with increasing accumulative inscription fluence reveals that the presence of boron enhances the photosensitivity of germanosilica fibers only slightly. In contrast, hydrogenation increases the refractive-index change by as much as an order of magnitude in fibers with high concentration of germanium. The presence of boron in hydrogenated fibers enhances significantly the photo-induced increase rate of the refractive index and results in FBGs with much wider bandwidths. The modulation depth of the photo-induced refractive-index change is stronger in hydrogenated boron co-doped fibers, thus making this fiber the best candidate for the inscription of gratings of high reflectivity. However, this type of fibers displays the highest excess loss among those examined; therefore, the choice of the appropriate fiber for FBG inscription depends on the application.

REFERENCES

1. K.O. Hill, B. Malo, F. Bilodeau, D.C. Johnson, and J. Albert, Bragg gratings fabricated in monomode photosensitive optical fiber by UV exposure through a phase mask, Appl Phys Lett 62 (1993), 1035–1037.
2. A. Arigiris, M. Konstantaki, A. Ikiades, D. Chronis, P. Florias, K. Kallimani, and G. Pagiatakis, Fabrication of high-reflectivity superimposed multiple-fiber Bragg gratings with unequal wavelength spacing, Optics Lett 27 (2002), 1306–1308.
3. J. Wang, Y. Dong, W. Cai, J. Yan, Y. Ma, X. Jia, M. Zou, and S. Xie, Optics Commun 200 (2001), 153–157.
4. X.Y. Dong, P. Shum, N.Q. Ngo, C.C. Chan, J.H. Ng, and C.L. Zhao, Largely tunable CFBG-based dispersion compensator with fixed center wavelength, Optics Express 11 (2003), 2970–2974.
5. A. Othonos, Fiber Bragg gratings, Rev Sci Instrum 68 (1997), 4309–4341.
6. D.L. Williams, B.J. Ainslie, J.R. Armitage, R. Kashyap, and R. Campbell, Enhanced UV photosensitivity in boron codoped germanosilicate fibers, Electron Lett 29 (1993), 45–47.
7. T. Erdogan, Fiber grating spectra, J Lightwave Technol 15 (1997), 1277–1294.
8. V. Finazzi and N. Zervas, Effect of periodic background loss on grating spectra, Appl Optics 41 (2002), 2240–2250.
9. J. Canning, M. Aslund, and P.-F. Hu, Ultraviolet-induced absorption losses in hydrogen-loaded optical fibres and in presensitized optical fibres, Optics Lett 25 (2000), 1621–1623.
10. P.J. Lemaire, R.M. Atkins, V. Mizrahi, and W.A. Reed, High-pressure H_2 loading as a technique for achieving ultrahigh UV photosensitivity and thermal sensitivity in GeO_2-doped optical fibers, Electron Lett 29 (1993), 1191–1193.
11. N.H. Ky, H.G. Limberger, R.P. Salathe, F. Cochet, and L. Dong, Hydrogen-induced reduction of axial stress in optical fiber cores, Appl Phys Lett 74 (1999), 516–518.

RADIATION CHARACTERISTICS OF CYLINDRICAL MICROSTRIP PHASED ARRAY ANTENNA MOUNTED ON ELECTRICALLY LARGE CYLINDER

Alexander Y. Svezhentsev
The A. Ya. Usikov Institute of Radio Physics and Electronics
National Academy of Sciences of Ukraine
12, Akad. Proskury str., 61085, Kharkov, Ukraine

Received 26 June 2004

ABSTRACT: *A problem of a microstrip cylindrical phased array antenna mounted on an electrically large cylinder is discussed. The array antenna consists of N patches, which are placed in the azimuthal plane. The solution is obtained by the method of moments (MoM) in the spatial domain using an improved representation of the spatial Green's function. In this representation, a leaky-wave contribution is extracted in addition to the previously extracted singularity at the origin and a surface-wave contribution.* © 2004 Wiley Periodicals, Inc. Microwave Opt Technol Lett 44: 152–157, 2005; Published online in Wiley InterScience (www.interscience.wiley.com). DOI 10.1002/mop.20573

Key words: *microstrip cylindrical phased-array antenna; Green's function; leaky-wave contribution*

1. INTRODUCTION

Conformal antennas are of great interest due to their ability to blend into curved surfaces. Antennas on cylindrical substrates (see Fig. 1) can be analyzed in a number of ways [1, 2], among which is the finite-element method, the method of auxiliary sources, the method of moments (MoM), and so forth. The MoM can be employed in both spectral [3] and spatial [4] domains. Both solutions work well if the cylinder is electrically small, that is, $r_0/\lambda_0 < 1$, where r_0 is the radius of the dielectric substrate (see Fig. 1), λ_0 is the free-space wavelength. If cylinder is electrically large ($r_0/\lambda_0 < 1$), the corresponding consideration presents problems and needs modifications.

Employment of the MoM in the spatial domain requires an effective algorithm to calculate the corresponding spatial Green's functions for sheet electrical-currents distributed on the surface of a dielectric-coated cylinder. In [5, 6], a new spatial Green's function has been obtained due to a special annihilating technique, which provides a singularity at the origin and a surface-wave contribution in explicit form. This Green's function has been already used to obtain some results for a single-patch problem in the case of an electrically small cylinder [4].

Firstly, in the present paper, a single-patch solution [4] is extended to an array of patches placed in the azimuthal plane. Secondly, some steps are made in an effort to advance the solution to electrically large cylinders. It turns out that an extension of the